Strong reversible Fe^{3+}-mediated bridging betwe dopa-containing protein films in water

Hongbo Zeng[a,b,2,1], Dong Soo Hwang[c,1], Jacob N. Israelachvili[b,2], and J. Herbert Waite[d,2]

[a]Department of Chemical and Materials Engineering, University of Alberta, Edmonton, AB, T6G 2V4 Canada; and [b]Department of Chemical Engineering, [c]Materials Research Laboratory, and [d]Department of Molecular, Cell and Developmental Biology, University of California, Santa Barbara, CA 93106

Contributed by Jacob N. Israelachvili, June 1, 2010 (sent for review February 10, 2010)

Metal-containing polymer networks are widespread in biology, particularly for load-bearing exoskeletal biomaterials. *Mytilus* byssal cuticle is an especially interesting case containing moderate levels of Fe^{3+} and cuticle protein—mussel foot protein-1 (mfp-1), which has a peculiar combination of high hardness and high extensibility. Mfp-1, containing 13 mol % of dopa (3, 4-dihydroxyphenylalanine) side-chains, is highly positively charged polyelectrolyte (pI ~ 10) and didn't show any cohesive tendencies in previous surface forces apparatus (SFA) studies. Here, we show that Fe^{3+} ions can mediate unusually strong interactions between the positively charged proteins. Using an SFA, Fe^{3+} was observed to impart robust bridging ($W_{ad} \approx 4.3$ mJ/m^2) between two noninteracting mfp-1 films in aqueous buffer approaching the ionic strength of seawater. The Fe^{3+} bridging between the mfp-1-coated surfaces is fully reversible in water, increasing with contact time and iron concentration up to 10 μM; at 100 μM, Fe^{3+} bridging adhesion is abolished. Bridging is apparently due to the formation of multivalent dopa-iron complexes. Similar Fe-mediated bridging ($W_{ad} \approx 5.7$ mJ/m^2) by a smaller recombinant dopa-containing analogue indicates that bridging is largely independent of molecular weight and posttranslational modifications other than dopa. The results suggest that dopa-metal interactions may provide an energetic new paradigm for engineering strong, self-healing interactions between polymers under water.

byssus | metal coordination | tris-catecholato-iron (III) complex

Metallopolymers are increasingly viewed as a transformative platform for the next generation of materials. This platform is related in part to their capacity for multifunctionality, but also to their wide and adjustable range of electronic, photonic, and magnetic properties (1). The load-bearing properties of metallopolymers are equally important but have received less attention with few exceptions (2). This oversight needs to be rectified given how widespread metal-containing polymer networks are in biology, particularly for load-bearing exoskeletal biomaterials (3, 4). The byssal cuticle of mussels in the genus *Mytilus* is an especially interesting case study because of its peculiar combination of hardness (100–150 MPa) and extensibility (>70% strain) (5). *Mytilus* byssal cuticle contains moderate levels of Fe^{3+} and a single protein—mussel foot protein-1 (mfp-1) (6). Mfp-1 has a mass of about 108 kDa in *Mytilus edulis* (7) and consists largely of tandem repeats of a positively charged decapeptide [AKPSYO*OTY*K], in which O, O*, and Y* denote *trans*-4-hydroxyproline, *trans*-2, 3, *cis*-3, 4-dihydroxyproline, and 3, 4-dihydroxyphenylalanine (dopa), respectively (8). At pH 7.5, purified mfp-1 forms stable tris- and bis-catecholate complexes ($\log K_s \sim 43$ at pH 7.5) with Fe^{3+} in solution by way of its dopa side chains (the tris form is shown in Fig. 1) (9, 10). Recently, resonance Raman microscopy has directly confirmed the presence of catecholato-Fe^{3+} complexes in the cuticle (11). Because the cohesive integrity of a polymeric material depends on the strength and density of its molecular interactions, it is critical to distinguish intermolecular from intramolecular Fe^{3+} complexation in mfp-1. A protein with a capacity for intermolecular metal complexation would be quite a novelty because, for nearly all the metalloproteins listed on the Brookhaven Protein Data Bank, metal binding is intramolecular (12).

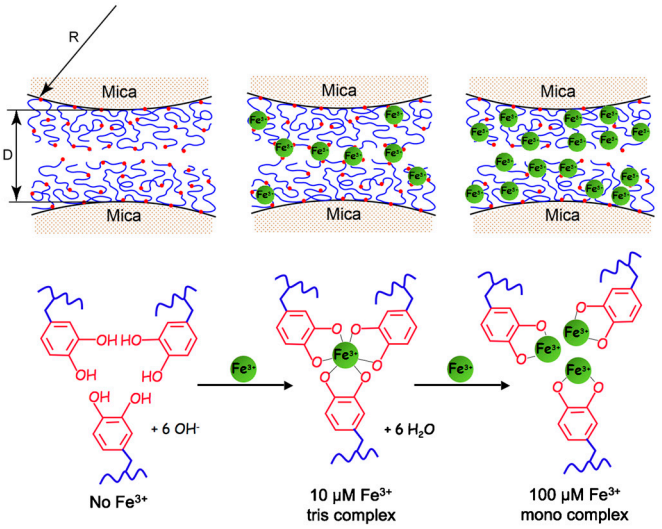


Fig. 1. The SFA experiments all involved symmetric deposition of mfp-1 on opposing mica surfaces. Before Fe^{3+} addition, the forces are normally repulsive or noninteracting (*Upper Left*). With the introduction of Fe^{3+}, however, there is strong bridging or attraction between the films (*Upper Center*). Bridging is due to multiple bidentate complexation of iron by dopa ligands (*Lower*). *D* is the distance between two mica surfaces; *R* is the radius of cylindrical curvature of the glued mica surfaces; red dots denote dopa residues.

We employed the surface forces apparatus (SFA) (13, 14) to assess the iron binding tendencies of mfp-1. Previous work reported that, despite strong adsorption to and the formation of hard walls on mica, mfp-1 showed weak to negligible adhesive bridging between two mica surfaces (15). This behavior is not inconsistent with the byssal coating function of mfp-1. However, mfp-1 molecules must be able to interact within the 5-μm-thick cuticle if the structure is to have cohesive strength. Dopa-Fe^{3+} complexation was previously proposed to provide "cure" in a crude extract of mussel foot proteins including mfp-1 (16).

To test the hypothesis that Fe^{3+} provides a cohesive bridge between adjacent mfp-1 molecules, we prepared equivalent mica surfaces with adsorbed mfp-1 (Fig. 1). Atomic force microscopy (AFM) imaging of mfp-1 coated mica before and after treatment with increasing iron reveals a finely patterned deposition that is roughened by metal binding (Fig. 2 *A*–*C*). Bridging between the

Author contributions: H.Z., D.S.H., J.N.I., and J.H.W. designed research; H.Z. and D.S.H. performed research; J.N.I. and J.H.W. contributed new reagents/analytic tools; H.Z. and D.S.H. analyzed data; and H.Z., D.S.H., J.N.I., and J.H.W. wrote the paper.

The authors declare no conflict of interest.

[1]H.Z. and D.S.H. contributed equally to this work.

[2]To whom correspondence may be addressed. E-mail: hongbo.zeng@ualberta.ca, waite@lifesci.ucsb.edu, or jacob@engineering.ucsb.edu.

This article contains supporting information online at www.pnas.org/lookup/suppl/doi:10.1073/pnas.1007416107/-/DCSupplemental.

Downloaded from https://www.pnas.org by CENTRAL SOUTH UNIVERSITY on November 9, 2026 from IP address 218.76.28.169.

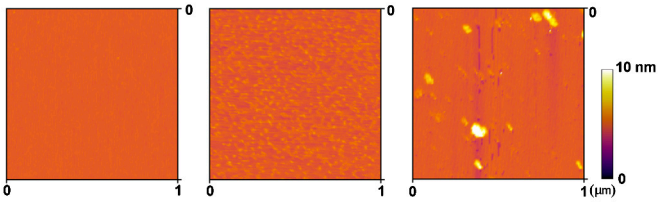


Fig. 2. AFM tapping mode images of mfp-1 films on freshly cleaved mica. (*A*) mfp-1 only; (*B*) mfp-1 with 10 μM Fe^{3+}; and (*C*) mfp-1 with 100 μM Fe^{3+}.

mfp-1 coated surfaces was investigated by the SFA in the absence and presence of Fe^{3+} at two different concentrations. Consistent with previous SFA results with mfp-1, no apparent bridging, i.e., attraction or adhesion between two mfp-1 coated mica surfaces was measured when two surfaces were brought into contact and separated immediately in 0.1 M sodium acetate (pH 5.5) (Fig. 3*A*). In contrast, in the presence of low Fe^{3+} (~10 μM), significant and reversible adhesion ($F_{ad}/R \sim -6$ mN/m) occurred when two mfp-1 layers were brought into contact and immediately separated (Fig. 3*B*). The adhesion increased to $F_{ad}/R \sim -8$ and -20 mN/m, respectively, for 10 and 100 min contact times (Fig. 3 *C* and *D*). At 10-fold higher concentrations (100 μM Fe^{3+}), however, bridging was abolished, i.e., F_{ad} was again zero (Fig. 4*A*).

The results suggest that, at low concentrations, Fe^{3+} provides significant cohesive bridges between mfp-1 molecules. The bridging is fully reversible, i.e., successive short contacts followed by separation all exhibited essentially identical bridging forces. Even additional contacts after a jump-out associated with a 100 min contact achieved up to 80% of the initial bridging force (Fig. S1).

The high pI and positive-charge density on mfp-1, coupled with the triply charged Fe^{3+}, make it unlikely that bridging iron is relying on electrostatic interactions as observed in the multivalent cation-mediated bridging of anionic polyelectrolyte films (17). Rather, multivalent dopa-metal chelate complexes are the more likely bridging structures (Fig. 1). If this hypothesis is correct, then bidentate dopa-Fe bridging should be detectable by resonance Raman spectroscopy (9) and abolished by a chelating agent such as EDTA. Resonance Raman peaks (550, 596, and 637 cm^{-1}) indicative of catechol-Fe complexes were detected

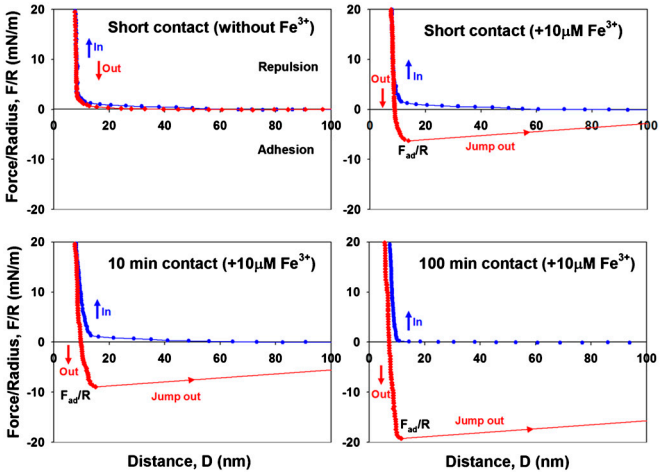


Fig. 3. Iron mediated bridging adhesion in symmetric mfp-1 films on mica. (*A*) short contact without Fe^{3+}; (*B*) short contact following 10 μM Fe^{3+} addition; (*C*) 10 min contact with added 10 μM Fe^{3+}; and (*D*) 100 min contact with added 10 μM Fe^{3+}. *D* and *R* are defined in Fig. 1, where $R \approx 2$ cm is the cylindrical radius of each surface in the "crossed-cylinder" geometry of the experiments. The adhesion and surface energies, $W_{ad} = 2\gamma$, are related to the measured force F_{ad} by $F_{ad}/R = (1.5-2)\pi W_{ad} = (3-4)\pi\gamma$ (see *Methods*).

in mica sandwiches of mfp-1 films with 10 μM Fe^{3+} as prepared for SFA force runs (Fig. S2). Only repulsive forces were detected by SFA (i.e., $F_{ad} = 0$) following the treatment with ~10 μM EDTA solution at same ionic strength and pH (Fig. 4*B*), which is consistent with the greater affinity of EDTA for Fe^{3+} at pH 5.5 than dopa (6).

SFA analysis of a recombinant version of mfp-1 (rmfp-1) provided additional mechanistic insights of Fe^{3+} bridging. Rmfp-1 contains the same repeating positively charged decapeptide sequence as the native protein but has only 12 repeats compared with the 75 repeats in mfp-1; moreover, of the many posttranslational modifications in native mfp-1, only dopa is present in rmfp-1. Notably, the hard wall of adsorbed rmfp-1 is thicker and the adhesion is stronger than the corresponding values for native mfp-1 for 0 min contact (Fig. 5). Mica coated with rmfp-1 lacking dopa did not result in measurable bridging with or without added Fe in the SFA (Fig. S3). These results indicate that bridging involves dopa but may be independent of prolyl-directed posttranslational modifications and molecular weight. The thicker hard wall, however, suggests that some rmfp-1 may be aggregating to higher molecular weights during the introduction of dopa (18).

Our results indicate that the intrinsically poor bridging properties of mfp-1 in the SFA relative to other dopa-containing proteins can be overcome by the addition of Fe^{3+}. This result is consistent with reports that mfp-1 needs Fe^{3+} to form a cohesive cuticle in mussel byssus (6, 11). Fe^{3+} appears to have two faces as a mediator for protein-based adhesion: (*i*) at short times (≤100 min) and low Fe^{3+} to dopa ratios, it provides strong but reversible interactions; and (*ii*) at longer times, its redox activity contributes to dopa oxidation and cross-linking (16). We have directly demonstrated Fe^{3+} ion's excellent short-term properties. Presumably, the time dependence of the work of adhesion at 10 μM Fe^{3+} (Fig. 3) has to do with protein rearrangement required to make more triscatecholato-iron complexes (Fig. 1). We suggest that at 100 μM Fe^{3+}, the tris complexes collapse into nonbridging monocatecholato-iron (Fig. 1). The combination of high strength, reversibility, and extensibility is unlike any other interaction studied. The strength has been noted previously in the interaction of dopa with titania and ferric oxide surfaces (19) and may be related to the charge transfer that occurs between the catecholic moiety of dopa and the metal (20).

Defining adhesion *energy* per unit area, W_{ad}, between two flat surfaces, by $W_{ad} \sim F_{ad}/1.5\pi R$ (see *Methods*), (14, 21) the iron bridging strength for 100 min contact ($F_{ad}/R \sim -20$ mN/m) can be converted to adhesion energy of 4.3 mJ/m^2. This bridging strength is much greater than bridging force between another mussel adhesive protein, mfp-3s, and mica ($W_{ad} \sim 0.6$ mJ/m^2) (15), or cadherin ectodomains oriented on lipid bilayers ($W_{ad} \sim 0.8$ mJ/m^2) (22, 23), and is approximately half the adhesion energy between biotin and avidin layers ($W_{ad} \sim 10$ mJ/m^2) (14).

Iron bridging between mfp-1 layers also depends on the multivalency of Fe^{3+} with respect to dopa ligands. Fe^{3+} is typically hexadentate with an octahedral geometry (12). Because each

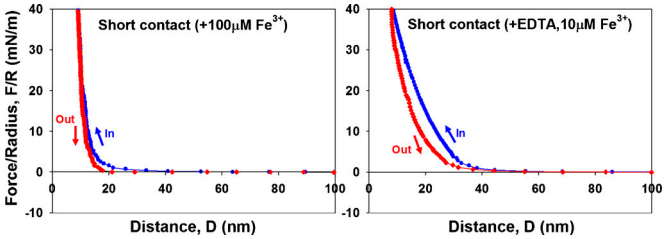


Fig. 4. Perturbations of Fe-mediated bridging: (*A*) film contraction and bridging loss at 100 μM Fe^{3+} (short contact); and (*B*) abolition of bridging at 10 μM Fe^{3+} by addition of 10 μM EDTA (short contact).

Downloaded from https://www.pnas.org by CENTRAL SOUTH UNIVERSITY on November 9, 2026 from IP address 218.76.28.169.

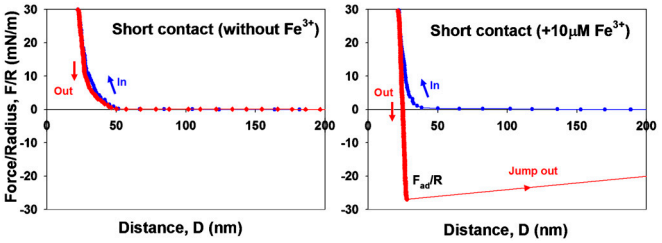


Fig. 5. Bridging adhesion in symmetric films of recombinant mfp-1 (rmfp-1) on mica. (*A*) Short contact without Fe^{3+}, and (*B*) short contact with added Fe^{3+}.

catechol is bidentate, Fe^{3+} can either bind one, two, or three dopa ligands. The actual number of ligands bound, however, is subject to equilibrium conditions and determined chiefly by the pH and the iron to dopa ratio (9, 24). The abolition of bridging at 100 μM Fe^{3+} is consistent with the formation of all monocatecholato-iron complexes, whereas in 10 μM Fe^{3+}, either bis- or tris-catecholate-Fe^{3+} complexes between layers would provide bridges.

Successful bridging by a smaller recombinant dopa-containing construct of mfp-1 is encouraging for future studies with recombinant proteins. Although it is reasonable to conclude that mfp-1 mimics need neither the non-dopa modifications nor the high mass in order to bridge with iron, mfp-1 is known to undergo measurable aggregation at pH 5 linked to spontaneous dopa oxidation (18). The extent to which aggregates are preferentially adsorbed to mica over the nonaggregated monomers needs to be further investigated.

Fe^{3+} bridging of dopa residues belonging to different polymer chains provides a spontaneous way to cross-link molecules under water. The cross-linking based on Fe^{3+} chelation is strong, reversible, and self-healing in the short term. In the long term and with redox exchange between oxygen, dopa, and Fe^{3+}, the bridging is likely to become less reversible with time, but this maturation needs greater scrutiny using Fe^{3+} as well as other nonredox-active metal ions. Metal-mediated bridging of macromolecules and their films has considerable potential for wet industrial and biomedical applications.

Methods

Mfp-1 Purification Mussel Feet. Mfp-1 was purified from frozen *M. edulis* feet according to published procedures (25). Sample purity was assessed by acid urea polyacrylamide gel electrophoresis, amino acid analysis, and MALDI-TOF mass spectrometry. The dopa in purified mfp-1 was typically ~12 mol % by amino acid analysis after a 1 h hydrolysis in 6 N HCl at 158 °C. Purified samples were freeze-dried and resuspended in a solution of 0.1 M sodium acetate buffer solution at pH 5.5, 0.25 M potassium nitrate, 1 mM Bis-Tris, and thereafter divided into convenient aliquot volumes for storage in aluminum-foil-covered vials at −50 °C prior to testing. Low pH and protection from light were necessary to reduce dopa losses in solution. The high salt concentration approaches seawater salinity. Milli-Q water (Millipore) was used for all glassware cleaning and solution preparation. Highest available purity ferric chloride and 2, 2′, 2″, 2‴-EDTA were obtained from Sigma-Aldrich.

Force vs. Distance Profiles Measurement by Surface Forces Apparatus. The normal force-distance profiles and adhesion forces of the mfp-1 were determined using an SFA in a configuration reported previously (14, 15). Basically, a thin mica sheet of 1–5 μm was glued onto a cylindrical silica disk (radius $R = 2$ cm). One-hundred microliters of mfp-1 solution (20 μg/mL) was injected onto one mica surface. Buffer conditions for all experiments were 0.1 M sodium acetate, 0.25 M potassium nitrate, and 1 mM Bis-Tris, pH 5.5. Bis-tris was added as a weak chelator of Fe^{3+}, thereby keeping the metal ion of $FeCl_3$ soluble and accessible to mfp-1 films (9). The buffer used in our experiments, namely 0.1 M sodium acetate with 0.25 M potassium nitrate at pH 5.5, differs notably in two respects from seawater (~0.56 M NaCl at pH 8.2): (*i*) buffer pH is lower to prevent dopa from oxidizing and mfp-1 and iron hydroxide from precipitating, and (*ii*) sodium chloride was substituted by potassium nitrate in the buffer solution to avoid corrosion of the semireflecting silver layers under the mica substrates, which normally occurs in high concentrations of chloride ions and affects the quality of the optical fringes. Contributions of electrostatic interactions to overall bridging are negligible with the buffering conditions used (26). The two curved and coated mica surfaces were then mounted in the SFA chamber in a crossed-cylinder geometry, which roughly corresponds to a sphere of radius R approaching a flat surface based on the Derjaguin approximation: $F(D) = 2\pi RW(D)$, where $F(D)$ is the force between the two curved surfaces and $W(D)$ the interaction energy per unit area between two flat surfaces. The measured adhesion or "pull-off" force F_{ad} is related to the adhesion energy per unit area W_{ad} by $F_{ad} = 2\pi RW_{ad}$ for rigid (undeformable) surfaces with weakly adhesive interactions, and by $F_{ad} = 1.5\pi RW_{ad}$ (used in this study) for soft deformable surfaces with strong adhesive contact (14, 27). All experiments were performed at room temperature (23 °C).

Recombinant Mussel Adhesive Protein Preparation in *Escherichia coli*. A recombinant cDNA corresponding to 12 tandem repeats of the mfp-1 consensus decapeptide $(AKPSYPPTYK)_{12}$ based on *E. coli's* codon preference was synthesized (Fig. S4) and cloned into pET28(+) vector for protein expression in *E. coli* using *Nco* I and *Hind* III restriction enzyme sites. The expected rmfp-1 sequence in the cloned vector was confirmed by DNA sequencing. The vector was inserted into *E. coli* [BL21(DE3)] and expression of rmfp-1 was performed by adding 1 mM of IPTG in the LB medium with kanamycin as a selection marker. Rmfp-1 was expressed in *E. coli* as inclusion bodies and solubilized by extraction in 5% acetic acid. Extracted rmfp-1 was purified by reversed phase HPLC (Aquapore RP-300 column 250 × 7.0 mm, Brownlee, Grace) using a flow rate of 1.0 mL/ min and an elution gradient described in a previous report (28). Purity of rmfp-1 (~95%) was confirmed by SDS-PAGE (Fig. S4) and amino acid analysis. Dopa-containing rmfp-1 was prepared by treatment of rmfp-1 with mushroom tyrosinase in borate buffer (29). The yield of dopa formation in rmfp-1 was estimated at 13 mol % by amino acid analysis.

AFM. Before imaging in air, three droplets of mfp-1 solution (pH 5.5) in the presence and the absence of 10 μM Fe^{3+} were placed on a freshly cleaved mica surface for about 20 min, then rinsed several times by buffer solution to remove excess proteins and by pure Milli-Q water to remove salt, and finally air dried in the laminar hood. Mfp-1-coated surfaces were inspected by AFM in tapping mode (Asylum, MFP-3D BIO, Asylum Research).

ACKNOWLEDGMENTS. We thank A. Masic of the Biomaterials Department at Max Planck Institute-Potsdam-Golm for the resonance Raman microprobe analysis and M. Tirrell for suggesting pertinent literature. We thank H. J. Cha for providing rmfp-1 cDNA. The work was substantially supported by the National Institutes of Health (R01 DE 018468) and the Materials Research Science and Engineering Centers Program of the National Science Foundation under Award DMR05-20415. D.S.H. acknowledges an Otis-Williams Fellowship.

1. Whittell GR, Manners I (2007) Metallopolymers: New multifunctional materials. *Adv Mater* 19:3439–3468.
2. Lee SM, et al. (2009) Greatly increased toughness of infiltrated spider silk. *Science* 324:488–492.
3. Broomell CC, et al. (2007) Mineral minimization in nature's alternative teeth. *J R Soc Interface* 4:19–31.
4. Lichtenegger HC, Birkedal H, Waite JH (2008) Heavy metals in the jaws of invertebrates. *Biomineralizatiom. From Nature to Application*Metal Ions in Life Sciences, eds A Sigel, H Sigel, and RKO Sigel pp 213–259.
5. Holten-Andersen N, Fantner GE, Hohlbauch S, Waite JH, Zok FW (2007) Protective coatings on extensible biofibres. *Nat Mater* 6:669–672.
6. Holten-Andersen N, et al. (2009) Metals and the integrity of a biological coating: The cuticle of mussel byssus. *Langmuir* 25:3323–3326.
7. Deacon MP, Davis SS, Waite JH, Harding SE (1998) Structure and mucoadhesion of mussel glue protein in dilute solution. *Biochemistry* 37:14108–14112.
8. Taylor SW, Waite JH, Ross MM, Shabanowitz J, Hunt DF (1994) Trans-2,3-cis-3,4-dihydroxyproline, a new naturally-occurring amino-acid, is the 6th residue in the tandemly repeated consensus decapeptides of an adhesive protein from *Mytilus-edulis*. *J Am Chem Soc* 116:10803–10804.
9. Taylor SW, Chase DB, Emptage MH, Nelson MJ, Waite JH (1996) Ferric ion complexes of a dopa-containing adhesive protein from *Mytilus edulis*. *Inorg Chem* 35:7572–7577.
10. Taylor SW, Luther GW, Waite JH (1994) Polarographic and spectrophotometric investigation of iron(III) complexation to 3,4-dihydroxyphenylalanine-containing peptides and proteins from *Mytilus-edulis*. *Inorg Chem* 33:5819–5824.
11. Harrington MJ, Masic A, Holten-Andersen N, Waite JH, Fratzl P (2010) Iron-clad fibers: A metal-based biological strategy for hard flexible coatings. *Science* 328:216–220.
12. Holm RH, Kennepohl P, Solomon EI (1996) Structural and functional aspects of metal sites in biology. *Chem Rev* 96:2239–2314.

Downloaded from https://www.pnas.org by CENTRAL SOUTH UNIVERSITY on November 9, 2026 from IP address 218.76.28.169.

13. Israelachvili JN, Adams GE (1978) Measurement of forces between 2 mica surfaces in aqueous-electrolyte solutions in range 0–100 nm. *J Chem Soc Faraday Trans* 74:975–1001.
14. Helm CA, Knoll W, Israelachvili JN (1991) Measurement of ligand receptor interactions. *Proc Natl Acad Sci USA* 88:8169–8173.
15. Lin Q, et al. (2007) Adhesion mechanisms of the mussel foot proteins mfp-1 and mfp-3. *Proc Natl Acad Sci USA* 104:3782–3786.
16. Monahan J, Wilker JJ (2003) Specificity of metal ion cross-linking in marine mussel adhesives. *Chem Commun* 14:1672–1673.
17. Schneider C, et al. (2008) Microsurface potential measurements: Repulsive forces between polyelectrolyte brushes in the presence of multivalent counterions. *Langmuir* 24:10612–10615.
18. Haemers S, van der Leeden MC, Frens G (2005) Coil dimensions of the mussel adhesive protein Mefp-1. *Biomaterials* 26:1231–1236.
19. Lee H, Scherer NF, Messersmith PB (2006) Single-molecule mechanics of mussel adhesion. *Proc Natl Acad Sci USA* 103:12999–13003.
20. Karpishin TB, Gebhard MS, Solomon EI, Raymond KN (1991) Spectroscopic studies of the electronic-structure of iron(III) tris(catecholates). *J Am Chem Soc* 113:2977–2984.
21. Zeng H, Maeda N, Chen NH, Tirrell M, Israelachvili J (2006) Adhesion and friction of polystyrene surfaces around Tg. *Macromolecules* 39:2350–2363.
22. Leckband D (2008) Beyond structure: Mechanism and dynamics of intercellular adhesion. *Biochem Soc Trans* 36:213–220.
23. Sivasankar S, Brieher W, Lavrik N, Gumbiner B, Leckband D (1999) Direct molecular force measurements of multiple adhesive interactions between cadherin ectodomains. *Proc Natl Acad Sci USA* 96:11820–11824.
24. Avdeef A, Sofen SR, Bregante TL, Raymond KN (1978) Coordination chemistry of microbial iron transport compounds. 9. Stability-constants for catechol models of enterobactin. *J Am Chem Soc* 100:5362–5370.
25. Waite JH, Tanzer ML (1981) Polyphenolic substance of *Mytilus edulis*: Novel adhesive containing L-dopa and hydroxyproline. *Science* 212:1038–1040.
26. Israelachvili JN (1992) *Intermolecular and Surface Forces* (Academic, London), 2nd Ed, pp 213–259.
27. Johnson KL, Kendall K, Roberts AD (1971) Surface energy and contact of elastic solids. *Proc R Soc Lon Ser-A* 324:301–313.
28. Holten-Andersen N, Zhao H, Waite JH (2009) Stiff coatings on compliant biofibers: The cuticle of *Mytilus californianus* byssal threads. *Biochemistry* 48:2752–2759.
29. Taylor SW (2002) Chemoenzymatic synthesis of peptidyl 3,4-dihydroxyphenylalanine for structure-activity relationships in marine invertebrate polypeptides. *Anal Biochem* 302:70–74.

Downloaded from https://www.pnas.org by CENTRAL SOUTH UNIVERSITY on November 9, 2026 from IP address 218.76.28.169.